Biogeochemistry (2008) 88:47–62
DOI 10.1007/s10533-008-9193-8

ORIGINAL PAPER

Influence of bacteria and salinity on diatom biogenic silica dissolution in estuarine systems

Vincent Roubeix · Sylvie Becquevort · Christiane Lancelot

Received: 20 April 2007 / Accepted: 3 March 2008 / Published online: 21 March 2008

Abstract Dissolution of diatom biogenic silica ($bSiO_2$) in estuaries and its control by water salinity and bacteria were investigated using the river euryhaline species *Cyclotella meneghiniana* as a model. Laboratory-controlled bioassays conducted at different salinities with an estuarine bacteria inoculum showed a faster dissolution of diatom $bSiO_2$ at the lowest salinity where bacteria were the most abundant. However in another experiment, salinity increase clearly enhanced the dissolution of cleaned frustules (organic matter free). The presence of active bacteria might therefore predominate on the effect of salinity for freshly lysed diatoms whereas salinity might rather control dissolution of organic-matter-free frustule remains. Incubation of cultivated diatoms at different protease concentrations revealed that high proteolytic activities had little effect on $bSiO_2$ dissolution at a 1-month scale in spite of an efficient removal of organic matter from the frustules. Altogether it is hypothesized that bacterial colonization increases $bSiO_2$ dissolution by creating a microenvironment at the diatom surface with high ectoproteolytic activity but also via the release of metabolic byproducts since the presence of organic matter seems generally to facilitate diatom $bSiO_2$ dissolution.

Keywords Bacteria · Biogenic silica · Diatoms · Dissolution · Estuaries · Salinity

V. Roubeix (✉) · S. Becquevort · C. Lancelot
Ecologie des Systèmes Aquatiques, Université Libre de Bruxelles, Boulevard du Triomphe, CP-221, 1050 Bruxelles, Belgium
e-mail: vroubeix@ulb.ac.be

Introduction

The silicon cycle along the land–ocean continuum deserves much attention because diatoms have an absolute requirement for Si in dissolved form (DSi, silicic acid) to build their specific siliceous frustules (biogenic silica, $bSiO_2$) which surround and protect the cells. Diatoms are the basis of pelagic and benthic coastal food chains. A drop in DSi availability in the coastal sea relatively to the other major nutrients (N and P) reduces the development of diatoms in favor of nonsiliceous autotrophic flagellates which are less efficiently grazed by metazooplankton and are more likely to lead to undesirable eutrophication events (Officer and Ryther 1980; Billen et al. 1991).

Silicon delivery to the coastal zone depends on Si emission from the watershed and transformations in the river system and estuary. The river Si load to estuaries includes on average 16% of $bSiO_2$ (Conley 1997), mostly the frustules of freshwater diatoms grown along the river reaches and phytoliths. Several studies reported high mortality of phytoplankton at the head of estuaries because of salinity increase or decreased light availability due to higher turbidity

(Morris et al. 1978; Anderson 1986; Ragueneau et al. 2002). Indeed osmotic stress and low light availability lead to the death of the most sensitive species including some diatoms. A significant part of river $bSiO_2$ load might dissolve inside estuaries (Anderson 1986). Moreover estuarine diatoms can increase the estuarine $bSiO_2$ pool provided that light and nutrients are available and that residence time is long enough to enable their growth. The dissolution of the $bSiO_2$ built either in river or in estuary will ultimately determine the amount of DSi reaching the coastal sea.

The biogenic silica composing diatom frustules is amorphous and hydrated (SiO_2, nH_2O). The external surface of the frustule is covered by an organic matrix mainly composed of proteins (rich in Asp, Ser, Gly, and Thr), saccharides, and lipids (Hecky et al. 1973). $bSiO_2$ dissolution takes place at the solid–water interface and consists of the release of reactive Si whose bonding to the underlying silica lattice has been weakened by chemical reactions with the aqueous solution (Van Cappellen et al. 2002).

Among the abiotic factors controlling $bSiO_2$ dissolution, temperature, pH, aluminium, and salt concentration in solution were mostly studied. An increase of temperature, pH (over 6) or salinity was reported to enhance $bSiO_2$ dissolution (Kamatani 1982; Yamada and D'Elia 1984; Van Cappellen and Qiu 1997; Hurd 1983) whereas an increase in concentration of dissolved aluminium leads to higher incorporation of Al into diatom frustules and to a slower dissolution of $bSiO_2$ (van Bennekom et al. 1989; Van Cappellen et al. 2002).

Diatom characteristics and biotic factors were also shown to influence $bSiO_2$ dissolution considerably. Kamatani and Riley (1979) and Hurd and Birdwhistell (1983) highlighted the importance of $bSiO_2$ specific surface area, which varies considerably among diatom species (Dixit et al. 2001). Also the preserving effect against dissolution of the organic matrix covering the external surface of diatom frustules (Hecky et al. 1973) was evidenced by cleaning frustules via chemical or enzymatic treatments prior to dissolution measurements (Lewin 1961; Kamatani and Riley 1979; Bidle and Azam 2001; Rickert et al. 2002). Patrick and Holding (1985) related the dissolution of fresh diatom frustules to the hydrolytic activity of inoculated bacteria and suggested the triggering role of bacteria in the degradation of the protective organic matrix. In agreement, batch dissolution experiments seeded with marine bacteria showed that the $bSiO_2$ dissolution rate was increased when bacteria were colonizing diatoms, resulting in an elevated exoproteolytic activity (Bidle and Azam 2001).

The most typical feature of estuaries is the salinity gradient generated by the progressive mixing of freshwater and seawater. This salinity gradient has an impact on Si fluxes to the coastal zone since it influences the Si uptake by phytoplankton (Ragueneau et al. 2002) and modifies the interaction of DSi with suspended particulate matter (Bien et al. 1958). Along estuaries there are also changes in bacterial activities not only because freshwater bacteria are generally more abundant than marine ones but also because bacterial activity can be locally enhanced where intense remineralization of riverine organic matter takes place (Goosen et al. 1999; Troussellier et al. 2002; del Giorgio and Bouvier 2002).

Biotic and abiotic factors controlling the process of $bSiO_2$ dissolution in estuaries were investigated by conducting laboratory-controlled dissolution experiments. $bSiO_2$ derived from *Cyclotella meneghiniana*, a common freshwater euryhaline diatom (Shafik et al. 1997; Roubeix et al. 2007), was chosen as a model. Focus was given to: (1) the variations of $bSiO_2$ dissolution along an estuarine salinity gradient, (2) the effect of salinity on the dissolution of cleaned (organic-free) diatom frustules, and (3) the effect of proteolytic activity on the dissolution of diatom $bSiO_2$.

Materials and methods

Experimental setup

C. meneghiniana was isolated from the Schelde estuary. It was maintained in WH culture medium (Guillard and Lorenzen 1972) at 20°C with a 14:10 light cycle at 100 µmol m^{-2} s^{-1}. Artificial seawater (ASW) was prepared according to Harrison et al. (1980). All dissolution experiments were conducted in polycarbonate bottles, in the dark at 20°C and used *C. meneghiniana* as the diatom $bSiO_2$ source. For each of them, pH was measured and did not change substantially during dissolution. As described below, initial $bSiO_2$ concentration was estimated as well as

the evolution of DSi concentrations during incubations. Experiments were run during 25–50 days and they were generally stopped before completion of $bSiO_2$ dissolution.

Bioassays 1: diatom $bSiO_2$ dissolution at different salinities with estuarine bacteria

C. meneghiniana was grown at 20°C with a 14:10 light cycle at 18 µmol m^{-2} s^{-1}. The freshwater culture was progressively diluted (at a rate of 0.14 d^{-1}) with ASW enriched with WH culture medium so that the diatom experienced a gradual salinity increase without nutrient shortage. The light level and the salinity of the inflowing water were set in order to reproduce approximately summer conditions in the turbid, long-residence-time Schelde Estuary (Soetaert et al. 1994, Soetaert and Herman 1995). The culture was sampled at salinities 0.3, 4, and 12 and the samples were frozen at −80°C to kill the diatoms and produce diatom-derived $bSiO_2$. The thawed $bSiO_2$ samples were then inoculated at 10% volume with bacteria sampled at salinity 0.3, 4, and 12 in the Schelde estuary in September 2004. Bacteria samples were isolated by 0.8 µm filtration of estuarine water. In addition to Si measurements, bacteria counts were also performed in each bioassay along the time course.

Bioassays 2: dissolution of cleaned diatom frustules at different salinities

The effect of dissolved salts on the dissolution of diatom frustules was addressed by first suppressing two potentially interfering factors: the organic matter associated to the frustules and bacteria which might use this organic matter as a substrate. This was performed by removing organic matter from diatom frustules and by autoclaving.

A batch culture of *C. meneghiniana* at the end of the exponential growth phase was concentrated by sedimentation and centrifuged (5 min at 500 × *g*). The collected material was dried at 40°C and organic matter was removed from the dried diatoms using a low-temperature asher with pure oxygen (Bax et al. 1990). An equal mass of the cleaned frustules was added to sterile ASW at salinities 0.5, 5, 10, 20, and 35. The corresponding ionic strength I to each salinity was calculated from the composition of ASW:

$$I = \frac{1}{2}\sum_i c_i z_i^2,$$

where c_i and z_i are the concentration in mol l^{-1} and the charge of ion *i*, respectively.

The frustules were disaggregated by ultrasonication (3 × 30 s) before starting measurements. Preliminary tests showed that such a treatment did not break the frustules.

In the following the term 'fresh' will be used in opposition to 'cleaned' to refer to diatoms used directly from culture for experimentation without undergoing a cleaning treatment.

Bioassays 3: dissolution of fresh $bSiO_2$ with different protease concentrations

A batch culture of *C. meneghiniana* was concentrated by sedimentation at the end of the exponential growth phase. The material was washed by three cycles of centrifugation (10 min at 500 × *g*) and resuspension in sterile Si-free water. The resulting diatom concentrate was free of bacteria as checked by epifluorescence microscopy and the diatom cells were not damaged and still able to grow after inoculation in new medium. The culture was equally distributed in six polycarbonate bottles containing autoclaved diluted ASW and Pronase E (Sigma), a bacterial extract of proteases, whose concentration ranged from 10^{-5} to 10^{-1} U ml^{-1} (+control) on a log scale. In each bottle a cocktail of antibiotics (penicillin + streptomycin) was added at a concentration of 35 mg l^{-1} to prevent bacterial contamination and cycloheximid (Sigma) at 1 mg l^{-1} (final concentration) to speed up the lysis of *C. meneghiniana* cells. The number of naked frustules (appearing completely free of organic matter) was counted along the experiment making use of inverted microscopy (1,000× magnification). No cell aggregation was observed during the incubations.

Bioassays 4: comparative dissolution of fresh and cleaned diatom frustules

Identical $bSiO_2$ concentrations of fresh cells and cleaned frustules of *C. meneghiniana* were incubated in parallel in sterile ASW at salinity 0.3. DSi was

measured along the two incubations in order to compare the dissolution rates of the two sources of $bSiO_2$.

Analytical measurements

DSi and bSiO$_2$

For $bSiO_2$ and DSi determinations, 10 ml samples were filtered on 47-mm-diameter polycarbonate membrane filters (0.6 µm pore size, Nucleopore). Filters were stored at room temperature in sealed Petri dishes and filtrates were acidified with 0.2% HCl suprapur and kept at 4°C until analysis. The $bSiO_2$ collected on filters was solubilized in 0.1 M NaOH at 100°C during 1 h and then neutralized with HCl 1 N (Paasche 1980). The solubilized $bSiO_2$ and DSi (filtrate) were analyzed spectrophotometrically at 810 nm using the silicomolybdate method (Grasshoff et al. 1983). DSi standards were prepared at the same salinity as the samples to avoid salinity interference on coloration. The relative standard deviation on $bSiO_2$ measurements was estimated to be 7% ($n = 13$).

Bacterial biomass

Samples for bacterial analyses were preserved with 40% buffered formaldehyde (final concentration 2%). Bacteria were filtered through 0.2 µm black Nuclepore polycarbonate filters of 25 mm diameter and stained by with 4′-6-diamidino-2-phenylindole (DAPI, final concentration 2.5 µg ml^{-1}) according to Porter and Feig (1980). A minimum of 1,000 cells were counted with a Leica epifluorescence microscope in at least ten different fields at 1,000× magnification. A relative standard deviation of 15% ($n = 20$) was estimated on bacterial abundance determination. Bacterial biovolumes were determined by image analysis (Lucia 4.6 software) and calculated by treating rods and cocci as cylinders and spheres, respectively (Watson et al. 1977). They were converted to carbon biomass by using the relation established from data measured by Simon and Azam (1989):

$$C = 0.12V^{0.72},$$

where C is the carbon per cell (pgC µm^{-3}) and V is the biovolume (µm^3).

Proteolytic activity

Proteolytic activity was determined fluorimetrically (Kontron SFM 25 fluorimeter) as the maximum hydrolysis rate of model substrates for leucine-aminopeptidase (L-leucine-7-amido-4-methyl-coumarin) added at saturating concentration (40 mmol l^{-1}). Wavelengths for excitation and emission were 360 and 445 nm for 7-amino-4-methylcoumarine (MCA). Fluorescence in the samples was measured as a function of time over 60 min at 20°C in the dark. Increase of fluorescent units with time was converted into activity from a standard curve prepared with the end product of the reaction, 7-amino-4-methylcoumarin (Sigma). The relative standard deviation was 12% ($n = 20$) on proteolytic activity measurements.

Particulate organic matter

Particulate organic carbon (POC) and nitrogen (PON) were determined by sample filtration on precombusted Whatman GF/F filters, drying the filters at 60°C, and analysis in a CNS NA 2000 Fisons auto-analyzer.

Dissolution rate calculations

According to Truesdale et al. (2005a) the $bSiO_2$ dissolution kinetics is described by plotting $\ln\frac{c_\infty - c_t}{c_\infty}$ as a function of time. In this relationship c_∞ and c_t are the DSi concentrations at times infinity and t, respectively, minus the initial DSi concentration in the solution. C_∞ equals the DSi concentration at equilibrium in solution when the initial $bSiO_2$ amount is several times more than its solubility (Truesdale et al. 2005a). In our experimental conditions, the solubility of $bSiO_2$ should be near 1,000 µM (Dixit et al. 2001). In every experiment the initial $bSiO_2$ concentration was low and DSi concentrations did not exceed 100 µM. Thus the dissolution rate was limited by $bSiO_2$ depletion and not by solution saturation. Therefore c_∞ can be replaced by p_0, the initial $bSiO_2$ concentration. Plotting $\ln\frac{(p_0 - c_t)}{p_0}$ versus time allows to identify linear portions which correspond to exponential dissolution phases. Indeed:

$$\frac{d\left[\ln\left(\frac{p_0 - c_t}{p_0}\right)\right]}{dt} = -K$$

is equivalent to:

$$\frac{dc_t}{dt} = K(p_0 - c_t) \quad (1)$$

and after integration:

$$c_t = p_0\left(1 - e^{-Kt}\right). \quad (2)$$

The apparent dissolution rate constants were graphically determined from the slope of the linear portions. For each dissolution experiment, one or two exponential phases could be identified and characterized by the constants K_1 and K_2. The biphasic kinetics might be the consequence of a heterogeneity in diatom $bSiO_2$ (Kamatani and Riley 1979; Truesdale et al. 2005b; see Discussion). However to compare the different bioassays in each experiment, only the apparent rate constants associated to the whole $bSiO_2$ were considered. Also, when the initial trend of dissolution was clear, the specific initial dissolution rate

$$K_0 = \frac{1}{p_0}\left(\frac{dc_t}{dt}\right)_{t=0}$$

(Greenwood et al. 2005) was also determined from the tangent at the origin of the plot of $\ln\frac{(p_0-c_t)}{p_0}$ versus time (Eq. 1).

The conditions of each experiment and the measured dissolution parameters are reported in Table 1.

Results

Diatom $bSiO_2$ dissolution under estuarine conditions

The time evolution of DSi at salinities 0.3, 4, and 12 showed differences in the dissolution kinetics (Fig. 1a–c) which were not related to the initial $bSiO_2$ stock (Table 1); for instance, the initial increase of DSi appeared to be the highest in the bioassay at salinity 0.3 (Fig. 1a), which had the lowest stock of $bSiO_2$ (Table 1). Comparison with Fig. 1d suggests that the high DSi release rate could be related to the higher bacteria inoculum at salinity 0.3, which allowed a fast bacterial development of approximately 0.5 mgC l^{-1} d^{-1} compared to 0.2 mgC l^{-1} d^{-1} at the two other salinities (Fig. 1d–f). In all our experiments, bacterial developments were rapidly controlled by the grazing of protozoa as revealed by epifluorescence microscopy. These grazers passed through the 0.8 μm pore filter and were unintentionally inoculated into the bioassays together with the estuarine bacteria. As reported by Bidle and Azam (1999), protozoa-mediated dissolution is negligible, nevertheless protozoa have an indirect effect in controlling bacterial communities.

The time dependence of $\ln\frac{(p_0-c_t)}{p_0}$ suggests that the DSi dissolution in each bioassay proceeded in two stages characterized by two apparent rate constants (Fig. 1g–i): a fast dissolution one (K_1) and a slower dissolution one (K_2) (Table 1). The shift in rate occurred when ~40% of initial $bSiO_2$ was dissolved. Comparison of the three bioassays showed a higher rate constant K_1 at salinity 0.3 with a value of 0.084 d^{-1} (Table 1). At salinity 4 and 12 the constants K_1 had closer values of 0.040 and 0.025 d^{-1}, respectively. Similarly K_2 was higher at salinity 0.3 (0.024 d^{-1}) than at salinity 12 (0.010 d^{-1}), but K_2 could not be estimated at salinity 4 because of highly scattered data (Fig. 1h). pH was close to neutrality in the three bioassays (Table 1).

Effect of salinity on the dissolution of cleaned diatom frustules

The effect of salinity on the dissolution of cleaned frustules is shown in Fig. 2, which plots $\ln\frac{(p_0-c_t)}{p_0}$ as a function of time for the different tested salinities. Dissolution was faster at salinity between 10 and 35, and could be entirely described by one apparent rate constant K_1 (Fig. 2). However at salinity 0.5 and 5 the kinetics was best described by two apparent rate constants K_1 and K_2 (Table 1) with K_2 being one order of magnitude lower than K_1. $bSiO_2$ dissolution at salinity 0.5 was almost stopped after 8 days, resulting in an extremely low K_2. The apparent rate constant K_1 had the lowest value at salinity 0.5 (0.005 d^{-1}) and the highest at salinity 20 (0.039 d^{-1}), whereas the values where similar at the other salinities (Table 1). Thus $bSiO_2$ dissolution rate was maximal at intermediate salinity and ionic strength (0.4 mol l^{-1}) between freshwater and seawater (Fig. 3). The pH varied between 6.8 and 7.8 for the different bioassays with higher values at higher salinities (Table 1).

Effect of proteases on the dissolution of fresh diatom $bSiO_2$

Figure 4 plots $\ln\frac{(p_0-c_t)}{p_0}$ as a function of time for different fresh diatom incubations in the presence of

Table 1 Bioassays experimental conditions and estimated specific initial dissolution rate (K_0) and apparent dissolution rate constants (K_1 and K_2) derived from linear regressions

Bioassays	Diatom derived $bSiO_2$	Initial $bSiO_2$ ($\mu mol\ l^{-1}$)	Salinity	Ionic strength ($mol\ l^{-1}$)	pH	Bacterial inoculum	Added proteases ($U\ ml^{-1}$)	Proteolytic activity ($\mu mol\ l^{-1}\ h^{-1}$)	K_0 (d^{-1})	K_1 (r^2) (d^{-1})	K_2 (r^2) (d^{-1})
1	Fresh	24	0.3	–	7.34	From estuary (sal 0.3)	0	nd	nd	0.084 (0.907)	0.024 (0.949)
	Fresh	23	4.0	–	7.46	From estuary (sal 4)	0	nd	nd	0.040 (0.959)	nd
	Fresh	34	12.0	–	7.55	From estuary (sal 12)	0	nd	nd	0.025 (0.936)	0.010 (0.942)
2	Cleaned	15	0.5	0.01	6.9	No	0	0	nd	0.005 (0.865)	0.000 (0.774)
	Cleaned	15	5.0	0.10	6.81	No	0	0	nd	0.016 (0.966)	0.004 (0.941)
	Cleaned	15	10.0	0.20	6.75	No	0	0	nd	0.017 (0.985)	
	Cleaned	15	20.0	0.40	7.28	No	0	0	nd	0.039 (0.992)	
	Cleaned	15	35.0	0.71	7.76	No	0	0	nd	0.020 (0.992)	
3	Fresh	120	10.0	0.20	6.74	No	0	0	0.027	0.034 (0.984)	0.025 (0.971)
	Fresh	120	10.0	0.20	6.75	No	10^{-5}	1	0.032	0.028 (0.998)	0.023 (0.973)
	Fresh	120	10.0	0.20	6.77	No	10^{-4}	10	0.034	0.034 (1.000)	0.022 (0.998)
	Fresh	120	10.0	0.20	6.78	No	10^{-3}	8.3×10^{1}	0.034	0.029 (0.991)	0.018 (0.985)
	Fresh	120	10.0	0.20	6.76	No	10^{-2}	9.2×10^{2}	0.040	0.029 (0.990)	0.015 (0.994)
	Fresh	120	10.0	0.20	6.78	No	10^{-1}	6.9×10^{3}	0.067	0.032 (0.974)	0.013 (0.976)
4	Fresh	40	0.3	0.01	7.02	No	0	0	nd	0.008 (0.989)	0.004 (0.972)
	Cleaned	40	0.3	0.01	6.94	No	0	0	nd	0.001 (0.849)	

r^2, squared correlation coefficient; nd, not determined

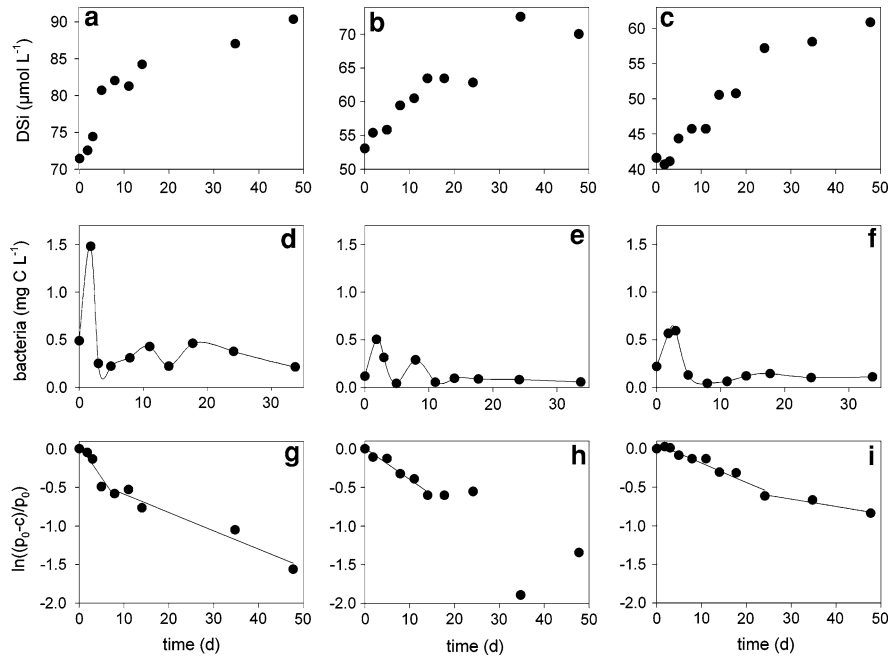

Fig. 1 Time evolution of DSi (**a**–**c**), bacterial biomass (**d**–**f**), and of $\ln\frac{(p_0-c_t)}{p_0}$ (**g**–**i**) for the dissolution of *C. meneghiniana*'s frustules in the presence of estuarine bacteria at salinities 0.3 (**a**, **d**, **g**), 4 (**b**, **e**, **h**), and 12 (**c**, **f**, **i**) (bioassays 1)

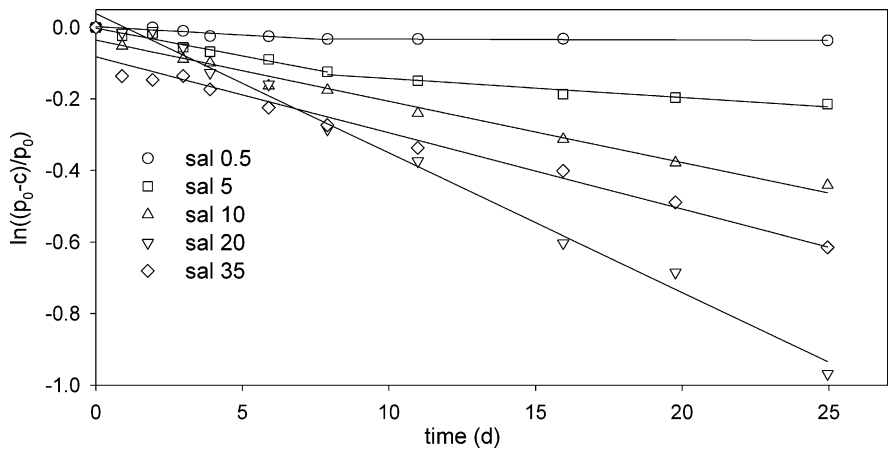

Fig. 2 Plots of $\ln\frac{(p_0-c_t)}{p_0}$ versus time for the incubations of cleaned *C. meneghiniana*'s frustules at different salinities (bioassays 2)

increased concentrations of proteases. For all concentrations, the kinetics of $bSiO_2$ dissolution showed a two-stage process (Fig. 4) characterized by two apparent rate constants K_1 and K_2. The value of K_1 was around 0.03 d^{-1} and did not show clear variations whereas K_2 decreased continuously with proteolytic activity up to one half of the control value in the incubation with the highest protease concentration (Fig. 5). For all the incubations we could estimate K_0, which showed a larger response than K_1 and increased with proteolytic activity resulting in a doubling between 10^2 and 10^4 µmol l^{-1} h^{-1} (Fig. 5).

Microscopy observations revealed a significant increase of the percentage of naked frustules in the two bioassays with the highest protease concentrations (Fig. 6). At the same time the PON:POC ratio, an indicator of the diatom protein content, decreased with rising protease concentration (Fig. 6). Altogether these two results reflected the hydrolysis of the diatom proteins by the enzymes added in solution. Interestingly, K_2 was positively correlated ($r^2 = 0.96$) to the PON:POC ratio measured on the 14th day of incubation (Fig. 7). For all the bioassays, pH was about 6.8 and was not affected by the different protease concentrations.

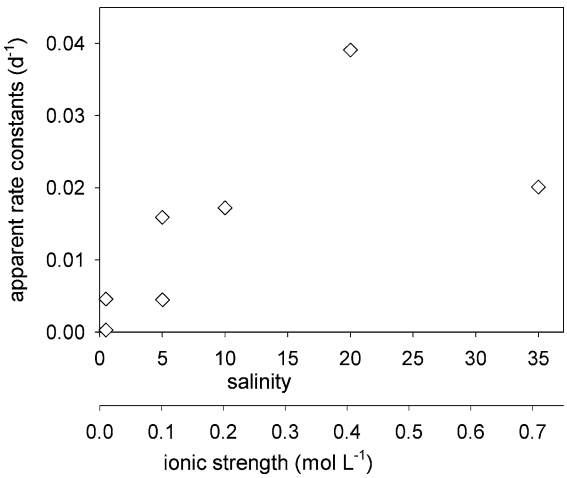

Fig. 3 Variations with salinity of the apparent $bSiO_2$ dissolution rate constants (◇) for the incubations of cleaned *C. meneghiniana*'s frustules (bioassays 2)

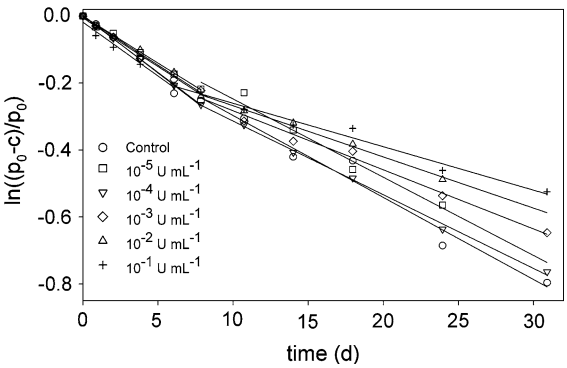

Fig. 4 Plots of $\ln\frac{(p_0-c_t)}{p_0}$ versus time for the incubation of fresh *C. meneghiniana*'s cells with increasing protease concentrations from 10^{-5} to 10^{-1} U ml^{-1} with control (bioassays 3)

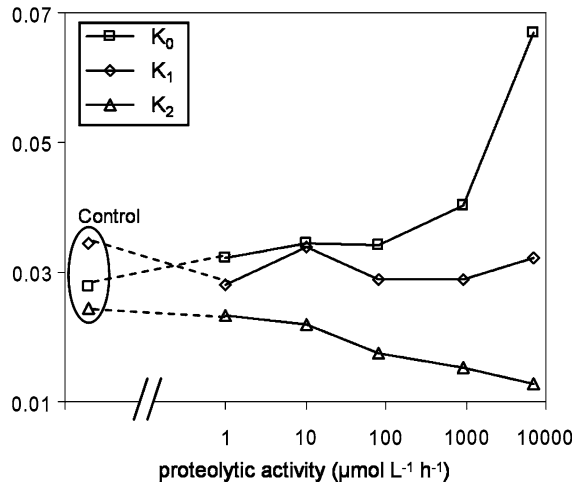

Fig. 5 Specific initial dissolution rate K_0 and apparent exponential dissolution rate constants K_1 and K_2 measured for fresh *C. meneghiniana*'s cells incubated at different proteolytic activities (PA) (bioassays 3)

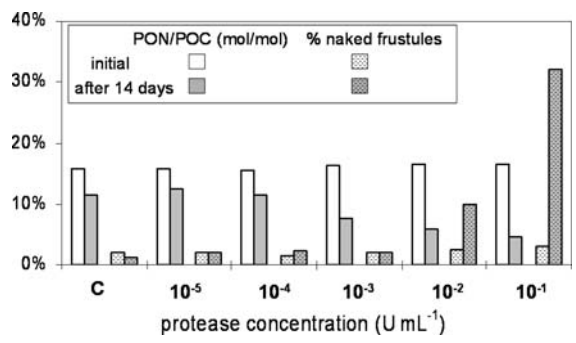

Fig. 6 Variations in the PON:POC ratio of *C. meneghiniana*'s cells and in the proportion of naked frustules after 2 weeks of incubation at different protease concentrations (bioassays 3)

Different dissolution of fresh diatom frustules and cleaned frustules

Figure 8 compares the time evolution of $\ln\frac{(p_0-c_t)}{p_0}$ for an identical $bSiO_2$ stock of fresh diatoms and cleaned frustules at salinity 0.3, in the absence of bacteria and added proteases. Clearly $bSiO_2$ from fresh diatoms dissolved faster than cleaned frustules obtained after removal of organic matter (Fig. 8). The estimated apparent dissolution rate constants K_1 and K_2 describing the two stages of the dissolution of the fresh diatom frustules were higher than the single rate constant K_1 measuring the dissolution of the cleaned frustules (Table 1).

Discussion

$bSiO_2$ dissolution model

For each $bSiO_2$ dissolution experiment, apparent rate constants were estimated using an exponential decay model (Eq. 2). Such a model simply expresses that $bSiO_2$ dissolution is proportional to the amount of $bSiO_2$ present in solution (Eq. 1).

However $bSiO_2$ dissolution is a complex process which is still not well understood. According to Van Cappellen et al. (2002) the time evolution of DSi concentration (c) in a batch reactor resulting from the dissolution of a concentration p of particulate

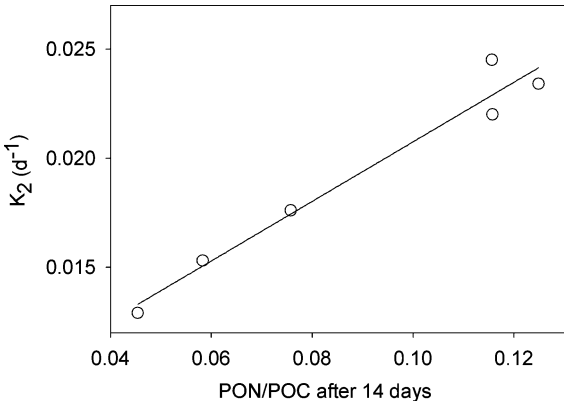

Fig. 7 Relation between the apparent dissolution rate constant K_2 and the PON:POC ratio after 14 days in the incubations of *C. meneghiniana*'s cells with different protease concentrations ($r^2 = 0.96$)

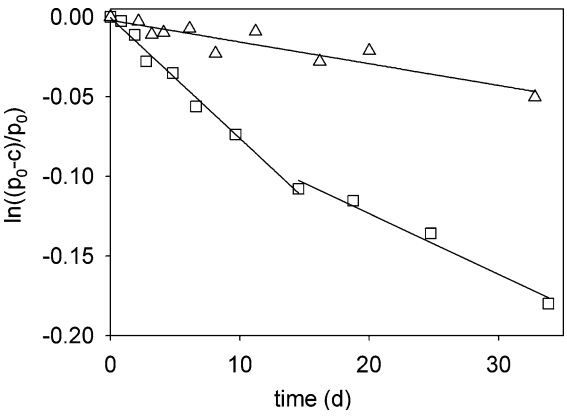

Fig. 8 Plots of $\ln\frac{(p_0-c_t)}{p_0}$ versus time for the incubations of fresh *C. meneghiniana*'s cells (without bacteria) and cleaned frustules at salinity 0.3 (bioassays 4)

$bSiO_2$ is described by the phenomenological rate expression:

$$\frac{dc}{dt} = k_0 g A_s f\left(1 - \frac{c}{c_{eq}}\right)p, \tag{3}$$

where k_0 is the rate constant, A_s the specific reactive surface area, c_{eq} the $bSiO_2$ equilibrium solubility, g is a factor representing the possible effects of the solution on the surface reactivity of the solid, and f is a function expressing the saturation effect when c approaches c_{eq}. According to Dixit et al. (2001) the solubility of $bSiO_2$ at 20°C in marine water (1 atm) is near 1,000 µmol l^{-1}.

Batch experiments conducted by Kamatani and Riley (1979) showed that the dissolution of small amounts of diatom frustules was exponential (Eq. 2), often divided in two stages. Moreover the derived rate constants K_i were found to be independent of the initial $bSiO_2$ stock, validating the first-order model (Eq. 1) (see also Truesdale et al. 2005b).

According to Eq. 3 the rate constant K integrates several variables:

$$K = k_0 g A_s f\left(1 - \frac{c}{c_{eq}}\right) \tag{4}$$

The derivation of a constant K on a time interval of dissolution assumes that g, A_s and $f(1 - c/c_{eq})$ have moderate variations (Hurd and Birdwhistell 1983). In particular c has to remain much lower than c_{eq}. In our experiments, DSi concentrations were low and did not exceed 100 µM, which is consistent with conditions in the water column of an estuary.

Some deviations from the first-order model (Eq. 2) were sometimes observed in batch dissolution as the rate constant K changed with different initial $bSiO_2$ concentrations (Greenwood et al. 2001; Truesdale et al. 2005a). Although this observation was not general (Greenwood et al. 2005), we attempted to set an equal initial $bSiO_2$ concentration in each bioassay of the same experiment (Table 1).

The empirical division of the kinetics in two exponential stages has been attributed to the differential dissolution of two parts in diatom frustules (Kamatani and Riley 1979). In agreement, Truesdale et al. (2005a) proposed the application of a sum of exponentials model to account for the heterogeneity of diatom $bSiO_2$:

$$c_t = p_0\left\lfloor f\left(1 - e^{-k_f t}\right) + (1-f)\left(1 - e^{-k_s t}\right)\right\rfloor \tag{5}$$

where f is the fraction of the fast dissolving part, k_f and k_s the rate constants associated to the fast and slow dissolving parts, respectively.

According to this model, the absolute value of the initial gradient of the plot $\ln\frac{(p_0-c_t)}{p_0}$ is the weighted average of the dissolution rate constants of both parts. Moreover the absolute value of the gradient of the second stage of dissolution tends to the dissolution rate constant of the slower dissolving part k_s:

$$\ln\left(\frac{p_0 - c}{p_0}\right) = \ln\left(f e^{-k_f t} + (1-f)e^{-k_s t}\right).$$

Then, the gradient G is:

$$G(t) = \frac{\mathrm{d}\left[\ln\left(\frac{p_0 - c_t}{p_0}\right)\right]}{\mathrm{d}t} = -\frac{fk_f e^{(k_s - k_f)t} + k_s(1-f)}{fe^{(k_s - k_f)t} + (1-f)}$$

particularly:

$$G(0) = -(fk_f + (1-f)k_s) \quad (6)$$

and as $k_s \leq k_f$, $G(+\infty) = -k_s$.

This model allows to interpret the two apparent rate constants K_1 and K_2 as approximations of the average dissolution rate constant of two parts of the diatom frustules and the rate constant of the slower dissolving part, respectively. K_0 is then a better estimation of the average dissolution rate constant of the heterogeneous $bSiO_2$ than K_1, especially when the first stage of dissolution does not appear clearly as a line passing through the origin on the plot of $\ln\frac{(p_0 - c_t)}{p_0}$ versus time (Truesdale et al. 2005b). The estimation of the three parameters of the model requires a precise data set and is as difficult as f approaches 0 or k_f and k_s converge.

The use of the sum of exponentials model can give additional information on the proportion of the fast dissolving fraction of $bSiO_2$ and the real rate constant associated to each part. The application of this model to bioassays 2 and 3 (Table 2) allowed the estimation of f, k_f and k_s characterizing the dissolution of *C. meneghiniana*'s frustules (Fig. 9). Application of the model improved the data fit for both bioassays especially at the beginning of dissolution and at the transition from one stage to the other (Fig. 9a and b to be compared with Figs. 4 and 2 respectively). The derived dissolution rate constants (Table 2) allowed a mechanistic interpretation of the proteolytic activity in each $bSiO_2$ fraction (see below). Moreover it showed that the apparent dissolution set previously in one stage of the cleaned frustules at salinities higher than 5 (Table 1 and Fig. 2) could actually proceed in two stages (Fig. 9b) with a very fast dissolution of the smaller fraction (Table 2) as was already suggested by the low intercept of the linear regression at salinity 35 (Fig. 2).

The fraction f of fast dissolving $bSiO_2$ was estimated 0.13 for the fresh diatoms incubated at different protease concentrations and 0.11 for the cleaned frustules dissolving at various salinities (Table 2). These estimations are lower than the value of 0.58 found by Truesdale et al. (2005b) for the same species but similar to the value determined for

Table 2 Parameters of the sum of exponentials model applied to diatom $bSiO_2$ dissolution in different experiments

Diatom species	$bSiO_2$ sample	Salinity	Temperature (°C)	Bacteria	f	k_f (d^{-1})	k_s (d^{-1})	R^2	Reference
C. meneghiniana	Fresh	10	20	10^{-4} U ml^{-1} proteases	0.13	0.161	0.020	0.994	This study
	Fresh	10	20	10^{-3} U ml^{-1} proteases	0.13	0.189	0.017	0.997	
	Fresh	10	20	10^{-1} U ml^{-1} proteases	0.13	0.389	0.013	0.999	
	Cleaned	5	20	No	0.11	0.177	0.004	0.994	
	Cleaned	35	20	No	0.11	2.000	0.019	0.994	
C. meneghiniana	Fresh	Seawater	40	No	0.48	1.344	0.084		Truesdale et al. (2005b)
Coscinodiscus gigas	Fresh	34	8	Surface seawater bacteria	0.13	0.504	0.022		Truesdale et al. (2005b) from Kamatani (1982)
	Fresh	34	14		0.13	0.672	0.034		
	Fresh	34	20		0.13	1.219	0.072		

R^2, coefficient of determination associated to the nonlinear regression

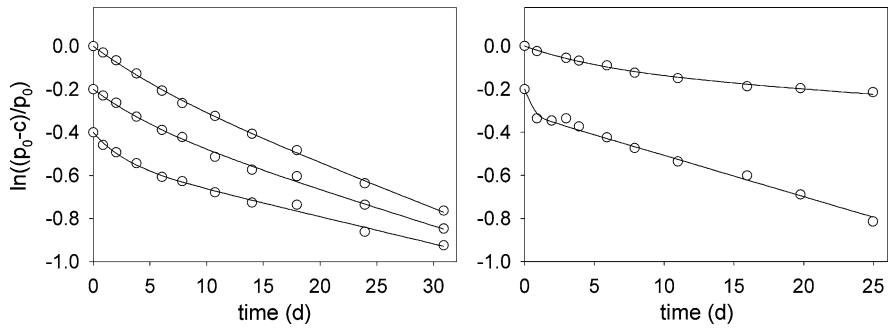

Fig. 9 Application of the sum of exponentials model (Truesdale et al. 2005a) to the dissolution data of (**a**) fresh diatom frustules at different protease concentrations and (**b**) cleaned frustules at two different salinities. On each graph, the curves are successively offset downwards by 0.2

Coscinodiscus gigas (0.13) by the same authors. More knowledge about the structure of diatom frustules and its variability would be needed to justify the distinction between two fractions characterized by different dissolution rates.

Meanwhile the apparent rate constants K_1 and K_2 were preferred to show the effect of the factors tested in this study on $bSiO_2$ dissolution because they do not require the difficult determination of the parameter f, which can be reasonably assumed to be the same for the different incubations of each experiment.

Comparison with other studies

Table 3 compares our K_1 and K_2 rate constants with literature values obtained at temperature equal or close to 20°C for marine diatoms, either fresh or cleaned from organic matter. Even if the values of K

Table 3 Literature review of exponential dissolution rate constants measured for different diatom species (all marine except for this study) at a temperature equal or close to 20°C

Diatom species	$bSiO_2$ sample	Temperature (°C)	K_1 (d^{-1})	K_2 (d^{-1})	Reference
Skeletonema costatum	Fresh	20	0.082		Kamatani (1969)
Thalassiosira decipiens	Fresh	22.7	0.0384		Kamatani and Riley (1979)
Rhizosolenia hebetata	Cleaned	22.7	0.408	0.0624	
Coscinodiscus gigas	Fresh	20	0.011		Kamatani (1982)
Coscinodiscus gigas	Cleaned	20	0.055	0.012	
Eucampia zodiacus	Fresh	20	0.050	0.022	
Eucampia zodiacus	Cleaned	20	0.18	0.058	
Chaetoceros deflandrei	Fresh	22	0.0125–0.0147		Tréguer et al. (1989)
Nitzschia cylindricus	Fresh	22	0.0156–0.0174		
Thalassiosira weissflogii	Fresh[a]	18	0.004–0.009		Bidle and Azam (2001)
Thalassiosira weissflogii	Fresh[b]	18	0.016–0.035		
Thalassiosira weissflogii	Cleaned[a]	18	0.051		
Chaetoceros decipiens	Fresh[a]	18	0.004–0.009		
Chaetoceros decipiens	Fresh[b]	18	0.026–0.051		
Chaetoceros decipiens	Cleaned[a]	18	0.073		
Cyclotella cryptica	Fresh	20[c]	0.023–0.029		Truesdale et al. (2005a)
Cyclotella meneghiniana	Fresh[a]	20	0.008–0.034	0.004–0.025	This study
Cyclotella meneghiniana	Fresh[b]	20	0.025–0.084	0.010–0.025	
Cyclotella meneghiniana	Cleaned[a]	20	0.005–0.039	0.000–0.005	

[a] Dissolution was measured without bacteria

[b] Dissolution was measured in the presence of living bacteria

[c] Dissolution rate constants initially determined at 40°C were corrected using the temperature function established by Kamatani (1982)

integrate variability of some intrinsic parameters such as A_s (Eq. 4) or f (Eq. 6) and some extrinsic factors linked to the experimental conditions such as pH or salinity (g in Eq. 4), our values compare well with the literature range. All studies do not report a K_2 value for diatom $bSiO_2$ dissolution. This can be explained by the high homogeneity of diatom $bSiO_2$ (Truesdale et al. 2005a) or by the focus given by the authors to the initial trend of dissolution. Interestingly, for the same diatom species, the cleaning of $bSiO_2$ induced a two-stage dissolution while the dissolution of the fresh cells could be described by only one rate constant K_1 (Kamatani 1982). Such an effect of the cleaning treatment on the dissolution kinetics was not observed in our experiments. When reported, the K_2 value was always lower than K_1 (on average $K_1 = 3.6K_2$). K_1 averaged 0.03 ± 0.02 d^{-1} for fresh diatoms and was clearly higher for cleaned frustules (0.15 ± 0.15 d^{-1}). Indeed several studies demonstrated a faster dissolution after the cleaning of the diatoms (Kamatani 1982; Bidle and Azam 2001; Rickert et al. 2002). On the contrary, in the present study the comparative dissolution of fresh and cleaned frustules at salinity 0.3 indicated a faster dissolution of fresh diatom $bSiO_2$. This could be explained by the strong reduction of dissolution at low salinity. All the literature measurements were made at seawater salinity. In bioassays 2, $bSiO_2$ dissolution was sharply increased from salinity 10 with probably the very fast dissolution of a small fraction of $bSiO_2$ (Fig. 9b) that sampling frequency did not allow to measure. It is possible that at high salinity ($\geq$10), diatom organic matter slows down dissolution of the faster dissolving part of the frustule while it has the contrary effect at river salinity. Anyway before concluding on the effect of diatom-derived organic matter on $bSiO_2$ dissolution, it would be important to make sure that the thermochemical pretreatment of diatoms for the removal of organic matter does not alter $bSiO_2$ surface reactivity (Van Cappellen and Qiu 1997).

The effect of salinity

The removal of organic matter before measuring the dissolution rate of diatom frustules is not realistic since the dissolution of the frustules may start before bacteria have fully degraded diatom organic matter, as shown in bioassays 3. Nevertheless this procedure allows to study the particular effect of salinity on the dissolution process. The cleaning of diatom frustules from organic matter was extensively used for $bSiO_2$ dissolution estimates. Various procedures were used based on chemical oxidation in acid solution or enzymatic digestion, always at elevated temperature (60–100°C) (see Kamatani and Riley 1979; Barker et al. 1994; Rickert et al. 2002). In our experiments the preservation of the frustule integrity was optimized by dry and low-temperature ashing (van Bennekom et al. 1989; Vrieling et al. 1999).

The increase of the apparent dissolution rate constants of the diatom frustules from salinity 0.5 to 20 (Table 1) confirmed the catalyzing effect of salinity on $bSiO_2$ dissolution. Hurd (1983) reported a twofold increase of the dissolution rate constant from salinity 5 to 35. Results obtained in this study with *C. meneghiniana* frustules suggest a factor 4–5 (Table 2). In our experiments, pH increased by one unit in the investigated salinity range, reaching at salinity 35 the value of 7.8, which is close to marine waters pH. Marshall and Warakomski (1980) established that the solubility of amorphous silica is invariant up to pH 10, even at high salinity. However Greenwood et al. (2005) reported an exponential increase of the initial dissolution rate of *Cyclotella cryptica* frustules from pH 7 at 0.7 M NaCl. According to the latter study, the pH increase from 7 to 8 in our experiments should have induced a doubling of the dissolution rate. Hence the pH variations recorded in bioassays 2 (Table 1) cannot explain alone the observed dissolution enhancement, especially at the lowest salinities. Moreover these pH variations are not consistent with the observed drop of the $bSiO_2$ dissolution rate from salinity 20 to 35 (Table 1). It is more likely that the salts have a direct effect on the dissolution reaction. The precise effect of salinity on the $bSiO_2$ dissolution is not clearly understood yet. Contradictory results have been obtained on the individual effect of various dissolved salts on the solubilization of amorphous silica from respectively silica gel and natural sediment samples (Marshall and Warakomski 1980; Barker et al. 1994). Barker et al. (1994) suggested that the solubility of silica might be controlled by the ionic strength of the solution, which reduces the activity coefficient of free ions to a minimum between 0.5 and 1 and makes it increase at higher levels. This could explain the observed increase of the apparent dissolution rate constants

from salinity 0.5 up to 20 where the ionic strength equals 0.4 mol l^{-1} and the reduction of the dissolution rate at salinity 35 where the ionic strength is 0.7 mol l^{-1} (Table 1). This is supported by bioassays 2 with cleaned frustules but contrasts with results obtained with fresh diatoms (bioassays 1) suggesting that diatom $bSiO_2$ dissolved faster at salinity 0.3 than at salinity 12. Such results indicate the preponderant action of another factor on fresh diatom frustules dissolution.

The role of bacteria

The addition of estuarine bacteria to diatom samples collected at the same salinity in an artificial gradient (bioassays 1) provided realistic conditions for the estimation of the in situ remineralization rate of biogenic silica from diatom frustules. However such bioassays cannot give precise information on the factors controlling the dissolution because too many parameters changed at the same time: salinity, abundance, taxonomic composition, and associated activity of bacteria and physiological state of the diatoms. At salinity 0.3, 63% of the initial $bSiO_2$ was dissolved after 30 days, which corresponds well to the results of Patrick and Holding (1985) who reported 50–60% dissolution of $bSiO_2$ from a *C. meneghiniana* culture inoculated with lacustrine bacteria after the same incubation time. As the dissolution kinetics and bacterial biomass are very similar at salinities 4 and 12, the faster dissolution at salinity 0.3 can be attributed to the higher bacterial biomass and the high peak observed after the first days of the experiment. The bacterial inoculum at salinity 0.3 was sampled in the high-turbidity zone of the estuary where detrital organic matter accumulates and bacterial remineralization is intense (Goosen et al. 1999). These bacteria isolated from an environment with usually high concentrations of detrital organic matter may have been more efficient for the biodegradation of the incubated diatoms. It was indeed demonstrated that natural bacterial assemblages are not all equivalent for the biodegradation of diatom detritus (Bidle and Azam 2001).

The role of bacteria was investigated by the use of dissolved proteases to mimic their hydrolytic action. Bacterial ectoproteolytic enzymes were shown to be mostly responsible of the induction of diatom frustule dissolution by the enzymatic hydrolysis of proteins forming the diatom $bSiO_2$ matrix (Bidle and Azam 2001). In bioassays 3, the addition of proteases had little effect on the dissolution of the diatom frustules even at very high proteolytic activity (Fig. 4). Only the initial rates K_0 testified to the action of the proteases (Table 1). The latter might have increased the reactive surface area (A_s) of the frustules by removing their organic coating and accelerated the dissolution of one part of the $bSiO_2$. In spite of an efficient cleaning of the diatoms through the hydrolysis of the proteins (Fig. 7), the effect of bacterial proteases on $bSiO_2$ dissolution appears to be limited at a 1-month scale. Bidle and Azam (1999) also obtained only a 10% increase of the dissolution of *C. fusiformis* and *T. weissflogii* frustules after one week with an addition of Pronase E corresponding to our highest concentration. Such a concentration gave a proteolytic activity which is much over the range of 0–5 μmol l^{-1} h^{-1} measured in natural aquatic systems (Laurent and Servais 1995). Proteolytic activities as high as measured in these experiments can only be envisaged in the microenvironment around diatom detritus where high density of colonizing bacteria can give rise to elevated local ectoprotease concentrations (Bidle and Azam 1999). The fact that proteases alone do not reproduce the clear dissolution enhancement demonstrated by Patrick and Holding (1985) and Bidle and Azam (1999) after inoculation of bacteria in axenic diatom cultures means that bacteria do not catalyze $bSiO_2$ dissolution only via the action of their proteases and the removal of organic matter but also by other ways.

The decrease of the apparent dissolution rate constant K_2 observed with increasing proteolytic activity (Fig. 5 and Table 1) and proportion of naked frustules (Fig. 6) in combination with the positive correlation of K_2 with the protein content of diatoms (Fig. 7) suggests that diatom organic matter might facilitate $bSiO_2$ dissolution. The application of the sum of exponentials model (Truesdale et al. 2005b) to bioassays 3 data at three levels of protease concentration (Fig. 5) showed that increased protease concentration enhanced dissolution of only the fast dissolving part of the frustules (13% of $bSiO_2$) but reduced dissolution of the main $bSiO_2$ fraction (Table 2). Diatom-derived organic matter could generally enhance frustule $bSiO_2$ dissolution but it could have a surface blockage effect (coating) if $bSiO_2$ can dissolve faster because of its fragile structure and the

effect of solution properties (high g, Eq. 3). Such a hypothesis would also explain why, in our experiments, at low salinity and without bacteria, the cleaned frustules dissolved slower than the fresh diatom ones (Fig. 8).

Some comparisons can be made with silicate mineral dissolution. In a similar way, studies of silicate mineral dissolution showed that the presence of organic compounds increased solubility of quartz via a mechanism of complexation and mobilization of silica (Bennett and Siegel 1987). For diatom amorphous silica, the cytoplasmic content of the cells could increase the reactivity of the surface of the frustule. Then colonizing bacteria could potentially amplify this effect by decomposing organic matter in smaller organic metabolites with stronger complexing abilities and reaching high concentrations in the frustule microenvironment, as was shown for silicate minerals (Ullman et al. 1996). Hurd (1983) also suggested that colonizing bacteria might lower pH in the frustule microenvironment by respiration processes (CO_2 release) and consequently decrease $bSiO_2$ dissolution. Experimental results on silicate minerals suggest that, on the contrary, bacterial metabolic products (organic acids) could locally and directly enhance $bSiO_2$ dissolution.

The control of salinity and bacteria on $bSiO_2$ dissolution in estuaries

The relative contribution of salinity and bacterial activity on diatom $bSiO_2$ dissolution may evolve during the transformation process from the death of diatoms to the complete dissolution of their frustules. Bioassay results obtained in undersaturated waters in DSi (Fig. 1 and Table 1) suggest that the presence of active bacteria predominates on the effect of salinity just after diatom death. High density of active bacteria can be expected where massive mortality of freshwater phytoplankton takes place and releases high concentrations of biodegradable organic matter in the medium. In this context fast colonization of diatom surface by bacteria should significantly enhance $bSiO_2$ dissolution. The importance of bacteria in $bSiO_2$ dissolution may be decreased when diatoms lyse in a part of estuary where bacteria are less concentrated and potentially experience osmotic stress (Painchaud et al. 1995; Langenheder et al. 2003). Bacterial colonization of diatom surface ceases when all organic matter attached to frustules has been degraded. At that time salinity might be the preponderant factor acting on dissolution of organic-matter-free frustule detritus. This corroborates results of Ryves et al. (2006) who found that salinity was the best predictor of diatom frustules dissolution in freshwater and saline lake sediments. Similarly, higher silica retention in the sediments can be expected near the head of estuaries where low salinity limits dissolution rather than lower in estuaries where faster dissolution might prevent efficient preservation of silica.

Acknowledgements The present work has been performed in the scope of the EU Research Training Network Si-WEBS (contract N° EU/CT-2002-00218) and the project AMORE-III funded by the Belgian Programme "Science for Sustainable Development" under contract N° SD/NS/03A. Thanks are due to Koenraad Muylaert (K.U. Leuven, Campus Kortrijk) for providing us with algal cultures and to Socratis Loucaides (Department of Geochemistry, Utrecht University) for his help in the preparation of cleaned diatom frustules.

References

Anderson GF (1986) Silica diatoms and a freshwater productivity maximum in Atlantic coastal plain estuaries. Chesapeake Bay Estuar Coast Shelf Sci 22:183–197

Barker P, Fontes J-C, Gasse F et al (1994) Experimental dissolution of diatom silica in concentrated salt solutions and implications for paleoenvironmental reconstruction. Limnol Oceanogr 39:99–110

Bax D, Agterdenbos J, Saakes A (1990) Role of nitrogen in dry destruction by low-temperature ashing in a low-pressure oxygen atmosphere in a microwave plasma. Anal Chim Acta 233:321–324

Bennett P, Siegel DI (1987) Increased solubility of quartz in water due to complexing by organic compounds. Nature 326:684–686

Bidle KD, Azam F (1999) Accelerated dissolution of diatom silica by marine bacterial assemblages. Nature 397: 508–512

Bidle KD, Azam F (2001) Bacterial control of silicon regeneration from diatom detritus: significance of bacterial ectohydrolases and species identity. Limnol Oceanogr 46:1606–1623

Bien GS, Contois DE, Thomas WH (1958) The removal of soluble silica from fresh water entering the sea. Geochim Cosmochim Acta 14:35–54

Billen G, Lancelot C, Meybeck M (1991) N, P and Si retention along the aquatic continuum from land to ocean. In: Mantoura RFC, Martin J-M, Wollast R (eds) Ocean margin processes in global change. Wiley, Chichester, pp 19–44

Conley DJ (1997) Riverine contribution of biogenic silica to the oceanic silica budget. Limnol Oceanogr 42:774–777

del Giorgio PA, Bouvier TC (2002) Linking the physiologic and phylogenetic successions in free-living bacterial communities along an estuarine salinity gradient. Limnol Oceanogr 47:471–486

Dixit S, Van Cappellen P, van Bennekom AJ (2001) Processes controlling solubility of biogenic silica and pore water build-up of silicic acid in marine sediments. Mar Chem 73:333–352

Goosen NC, Kromkamp J, Peene J et al (1999) Bacterial and phytoplankton production in the maximum turbidity zone of three European estuaries: the Elbe, Westerschelde and Gironde. J Mar Syst 22:151–171

Grasshoff K, Erhardt M, Kremling K (1983) Methods of seawater analysis. Verlag Chemie, Weinheim

Greenwood JE, Truesdale VW, Rendell AR (2001) Biogenic silica dissolution in seawater—in vitro chemical kinetics. Prog Oceanogr 48:1–23

Greenwood JE, Truesdale VW, Rendell AR (2005) Toward an understanding of biogenic-silica dissolution in seawater—an initial rate approach applied between 40 and 90°C. Aquatic Geochem 11:1–20

Guillard RRL, Lorenzen CJ (1972) Yellow-green algae with chlorophyllide c. J Phycol 8:10–14

Harrison PJ, Waters RE, Taylor FJR (1980) A broad spectrum artificial medium for coastal and open ocean phytoplankton. J Phycol 16:28–35

Hecky RE, Mopper K, Kilham P et al (1973) The amino acid and sugar composition of diatom cell-walls. Mar Biol 19:323–331

Hurd DC (1983) Physical and chemical properties of siliceous skeletons. In: Aston SR (ed) Silicon geochemistry and biogeochemistry. Academic, London, pp 187–244

Hurd DC, Birdwhistell S (1983) On producing a more general model for biogenic silica dissolution. Am J Sci 283:1–28

Kamatani A (1969) Regeneration of inorganic nutrients from diatom decomposition. J Oceanogr Soc Japan 25:63–74

Kamatani A (1982) Dissolution rates of silica from diatoms decomposing at various temperatures. Mar Biol 68:91–96

Kamatani A, Riley JP (1979) Rate of dissolution of diatom silica walls in seawater. Mar Biol 55:29–35

Langenheder S, Kisand V, Wikner J et al (2003) Salinity as a structuring factor for the composition and performance of bacterioplankton degrading riverine DOC. FEMS Microbiol Ecol 45:189–202

Laurent P, Servais P (1995) Fixed bacterial biomass estimated by potential exoproteolytic activity. Can J Microbiol 41:749–752

Lewin JC (1961) The dissolution of silica from diatom walls. Geochim Cosmochim Acta 21:182–198

Marshall WL, Warakomski M (1980) Amorphous silica solubilities-II. Effect of aqueous salt solutions at 25°C. Geochim Cosmochim Acta 44:915–924

Morris AW, Mantoura RFC, Bale AJ et al (1978) Very low salinity regions of estuaries: important sites for chemical and biological reactions. Nature 274:678–680

Officer CB, Ryther JH (1980) The possible importance of silicon in marine eutrophication. Mar Ecol Prog Ser 3:83–91

Paasche E (1980) Silicon content of five marine plankton diatom species measured with a rapid filter method. Limnol Oceanogr 25:474–480

Painchaud J, Therriault J-C, Legendre L (1995) Assessment of salinity-related mortality of freshwater bacteria in the Saint Lawrence estuary. Appl Environ Microbiol 61: 205–208

Patrick S, Holding AJ (1985) The effect of bacteria on the solubilization of silica in diatom frustules. J Appl Bacteriol 59:7–16

Porter KG, Feig YS (1980) The use of DAPI for identification and enumeration of aquatic microflora. Limnol Oceanogr 25:943–948

Ragueneau O, Lancelot C, Egorov V et al (2002) Biogeochemical transformations of inorganic nutrients in the mixing zone between the Danube River and the northwestern Black Sea. Estuar Coast Shelf Sci 54:321–336

Rickert D, Schlüter M, Wallman K (2002) Dissolution kinetics of biogenic silica from the water column to the sediments. Geochim Cosmochim Acta 66:439–455

Roubeix V, Rousseau V, Lancelot C (2007) Diatom succession and silicon removal from freshwater in estuarine mixing zones: From experiment to modelling. Estuar Coast Shelf Sci. doi:10.1016/j.ecss.2007.11.007

Ryves DB, Battarbee RW, Juggins S et al (2006) Physical and chemical predictors of diatom dissolution in freshwater and saline lake sediments in North America and West Greenland. Limnol Oceanogr 51:1355–1368

Shafik HM, Herodek S, Voros L et al (1997) Growth of *Cyclotella meneghiniana* Kütz. I. Effects of temperature light and low rate of nutrient supply. Ann Limnol 33: 139–147

Simon M, Azam F (1989) Protein content and protein synthesis rates of planktonic marine bacteria. Mar Ecol Prog Ser 51:201–213

Soetaert K, Herman PMJ (1995) Estimating estuarine residence times in the Westerschelde (The Netherlands) using a box model with fixed dispersion coefficients. Hydrobiology 311:215–224

Soetaert K, Herman PMJ, Kromkamp J (1994) Living in the twilight: estimating net phytoplankton growth in the Westerschelde estuary (The Netherlands) by means of an ecosystem model (MOSES). J Plankton Res 16: 1277–1301

Tréguer P, Kamatani A, Gueneley S et al (1989) Kinetics of dissolution of antarctic diatom frustules and the biogeochemical cycle of silicon in the southern ocean. Polar Biol 9:397–403

Troussellier M, Schäfer H, Batailler N et al (2002) Bacterial activity and genetic richness along an estuarine gradient (Rhône river plume, France). Aquat Microb Ecol 28: 13–24

Truesdale VW, Greenwood JE, Rendell AR (2005a) In vitro, batch-dissolution of biogenic silica in seawater—the application of recent modelling to real data. Prog Oceanogr 66:1–24

Truesdale VW, Greenwood JE, Rendell A (2005b) The rate-equation for biogenic silica dissolution in seawater—new hypotheses. Aquatic Geochem 11:319–343

Ullman WJ, Kirchman DL, Welch SA et al (1996) Laboratory evidence for microbially mediated silicate mineral dissolution in nature. Chem Geol 132:11–17

van Bennekom AJ, Jansen JHF, van der Gaast SJ et al (1989) Aluminium-rich opal: an intermediate in the preservation

of biogenic silica in the Zaire (Congo) deep-sea fan. Deep-Sea Res 36:173–190

Van Cappellen P, Qiu L (1997) Biogenic silica dissolution in sediments of the Southern Ocean. II Kinetics. Deep-Sea Res II 44:1129–1149

Van Cappellen P, Dixit S, Gallinari M (2002) Biogenic silica dissolution and the marine Si cycle: kinetics, surface chemistry and preservation. Oceanis 28:417–454

Vrieling EG, Beelen TPM, van Santen RA et al (1999) Diatom silicon biomineralization as an inspirational source of new approaches to silica production. J Biotechnol 70:39–51

Watson SW, Novitsky TJ, Quinby HL et al (1977) Determination of bacterial number and biomass in marine environment. Appl Environ Microbiol 33:940–946

Yamada SS, D'Elia CF (1984) Silicic acid regeneration from estuarine sediment cores. Mar Ecol Prog Ser 18:113–118